Journal of Computational Physics **168,** 26–46 (2001)
doi:10.1006/jcph.2000.6676, available online at http://www.idealibrary.com on IDEAL®

Self-Consistent Description of Radial Space-Charge Confinement in DC Column Plasmas

M. Schmidt, D. Uhrlandt, and R. Winkler

Institut für Niedertemperatur-Plasmaphysik, 17489 Greifswald, Germany

Received December 2, 1999; revised October 20, 2000

A new method for the self-consistent description of radial space-charge confinement and the corresponding nonlocal kinetics of plasma components in the cylindrical dc column plasma is presented. The method comprises the solution of the space-dependent kinetic equation of the electron component, the fluid equations of ions and excited neutral particles and Poisson's equation. The nonlinearly coupled equations are solved self-consistently applying a nonlinear optimization technique, which is used to optimize a polynomial representation of the radial space-charge potential. The applicability of several optimization methods and their suitability concerning the convergence and accuracy are discussed. Examples of the self-consistent description are presented.

Key Words: dc column plasma; electron kinetics; Poisson's equation; function minimization.

1. INTRODUCTION

In recent years, a more accurate description and a deeper understanding of the spatial structure of collision-dominated low-pressure plasmas have been reached. This concerns in particular the kinetics of the plasma components in rf and dc glow discharge plasmas, where one source of the spatial nonuniformity is the plasma confinement by space charges in front of the insulated walls. Primarily, an effort has been made to treat more accurately the electron component in such plasmas. It has been shown that a nonlocal treatment of the electron kinetics is necessary if the plasma operates at pressures of a few Torr or below.

The comprehensive description of such plasmas should include, in addition, the adequate treatment of the ion and most important neutral components and the description of the space-charge fields and heating electric fields in the plasma. Moreover, the kinetics of the plasma components and the electric field has to be treated self-consistently, which requires generally the solution of nonlinearly coupled differential equations. To treat the nonlocal kinetics of the electron component, its space-dependent kinetic equation has to be

0021-9991/01 $35.00

solved. Most existing self-consistent models abstain from the solution of the corresponding complex partial differential equation by applying more or less simplified approaches to describe the nonuniform electron kinetics. The simplifications lead partly to a decoupling of the description of the electron energy distribution and the hydrodynamic treatment of the plasma components. Finally, only ordinary differential equations such as the fluid equations have to be solved to determine the densities and the fluxes of the plasma components and Poisson's equation to determine the space-charge field.

In this paper, the cylindrical positive column of a dc discharge is considered as a typical representative of a spatially bounded plasma. A new method for the self-consistent description of the space-charge confinement in the cylindrical dc column plasma is presented. The method comprises the accurate treatment of the nonuniform electron kinetics, the ion and excited atom kinetics, and the radial space charge field by solving the radially inhomogeneous electron kinetic equation, the balance equations of excited neutrals, the ion momentum balance, and Poisson's equation. These equations are self-consistently solved applying a nonlinear optimization technique to obtain the space-charge potential profile. The method does not include the determination of the axial field strength which, in addition, needs a detailed treatment of plasma-wall interaction processes. However, the accurate description of the space-charge confinement and of the nonuniform kinetics of plasma components represents a necessary step for the development of a complete self-consistent column plasma description.

After a brief presentation of several existing self-consistent models and their limitations, the basic assumptions to describe the space-charge confined plasma column are given in the second section. In the third section the numerical techniques, applied in the corresponding model, are described. The presentation is focussed on details of the optimization techniques and the solution of Poisson's equation. First results of the method are shown and discussed in Section 4.

Starting with the ambipolar diffusion theory of Schottky [1] in 1924, several models have been developed in the past to self-consistently describe the column plasma kinetics under the action of the radial space-charge confinement. In the following, the degree of limitations of these models is assessed according to two questions: How roughly simplified is the description of plasma components, in particular that of electrons? What methods are applied to solve Poisson's equation and to self-consistently determine the space-charge potential?

Many authors [1–4] abstained from the solution of Poisson's equation and used instead a rough estimation of the space-charge field assuming quasi-neutrality. Their self-consistent models should not be discussed in detail here. Most of the authors who solved Poisson's equation assumed a Maxwellian energy distribution of ions and electrons with constant ion and electron temperatures [5–10]. Instead of the kinetic equations they solved the moment equations, i.e., the fluid equations of electrons and ions coupled with Poisson's equation. The latter is called the moment method in the literature. A treatment of excited atom states and stepwise ionization processes were omitted in these models. Such models are not applicable to describe the nonequilibrium column plasma at lower pressure and lower electron density, where the electron energy distribution strongly deviates from a Maxwellian and distinctly varies with the radial position.

Initial improvements have been achieved by solving the spatially homogeneous Boltzmann equation instead of assuming a Maxwellian distribution for the electrons to determine ionization frequencies and transport coefficients as an input for the moment equations [11]. However, the radial dependence of the electron energy distribution has also been neglected in these models.

An extension of the moment method, which takes into account the radial variation of the electron temperature and the transport coefficients, has been developed recently by Ingold [12]. Here, in addition to the radial particle fluxes, a radial heat flux of electrons is described. The system of moment equations has been extended by the electron energy balance and the heat flux equation. The radially dependent electron transport coefficients—among others the diffusion coefficient and the mobility—and the collision frequencies are expressed as functions of the mean electron energy. These functions are obtained from the solutions of the homogeneous Boltzmann equation for an appropriate range of electric field strengths. This approach also avoids the solution of the radially inhomogeneous electron kinetic equation but in most cases yields better estimates of the transport coefficients. Stronger deviations are expected with respect to the treatment of the charge carrier production by this approach.

The accurate radial variation of the electron collision rates and transport coefficients can be obtained by the solution of the space-dependent electron kinetic equation only. A numerical solution of this equation to describe the electron kinetics in inhert gas dc column plasmas has been performed by several authors [4, 13–22] recently. Most of these approaches [4, 13, 15, 17–22] are based on the two-term expansion of the electron velocity distribution (EVD) into spherical harmonics. In the other approaches [14, 16], particle simulation techniques have been used to solve the kinetic equation. However, most of these authors assumed roughly simplified model functions for the radial space-charge potential [4, 15, 16, 19, 22, 23] or used a potential function resulting from corresponding electrical probe measurements [17, 18, 21].

Up to now, only some authors [4, 13, 14, 22, 23] have made initial attempts to apply a nonlocal electron kinetic treatment inside a self-consistent positive column model, which includes the determination of the radial space-charge field. Hartig and Kushner [13] deduced the radial field from the radial ambipolar flux avoiding the solution of Poisson's equation. Behnke *et al.* [4] and Golubovskii *et al.* [22, 23] started with an electron kinetic treatment for a given roughly simplified model potential and determined afterwards a new estimate of the potential assuming quasi-neutrality [4, 23] or solving Poisson's equation [22]. However, they did not consistently take into account the coupling of the equations by applying the resulting potential function in an additional treatment of the electron and ion kinetics. Furthermore, the applied treatment of the electrons is based on the so-called nonlocal approach [24] of the radially inhomogeneous kinetic equation and, consequently, represents an additionally simplified description of the space-dependent electron kinetics [18, 25].

Parker *et al.* [14] made first attempts to solve Poisson's equation self-consistently coupled with the description of the electron and ion kinetics by means of the convected scheme technique. This method is of excessive expenditure as mentioned in [16].

Except for the recent work of Golubovskii *et al.* [22], all these authors avoided the additional coupling of the electron kinetic treatment with a balancing of important excited atom states and described the charge carrier production very roughly by taking into account direct ionization of ground state atoms only. The self-consistent coupling of the spatially resolved treatments of the excited atom kinetics and the electron kinetics is described, in [17, 18, 21, 22].

2. BASIC ASSUMPTIONS OF THE MODEL

The column plasma of dc discharges in a pressure range between some tenths of a Torr and some Torr and of an ionization degree below about 10^{-5} is considered. The plasma

is bounded by an insulated cylindrical tube of radius r_w and is assumed to be rotationally symmetric, axially homogeneous, and time-independent. The axial discharge current I_z is carried by the electron flux driven by the constant axial electric field E_z, which supplies the plasma with power. The electric power is mainly absorbed by the electrons, which then can excite and ionize gas atoms. Consequently, besides the gas atoms in ground state with density N_0, several excited particle components, with densities $N_l(r), l = 1, 2, \ldots$ depending on the radial position r, occur in the plasma. The plasma is maintained by the production of charge carriers in the plasma volume, which is often dominated by the ionization of these excited particles. To simplify matters, it is assumed that only one species of single-charged ions with the density $n_i(r)$ exists in the plasma. According to the considered gas pressure range, the ion movement is assumed to be mainly mobility-limited. The electrons and ions tend to diffuse toward the wall, and, since the electrons have a much larger mobility, a positive charge excess develops in the plasma in the beginning of the discharge operation. Thus, a radial space-charge field $E_r(r)$ is builtup, which accelerates the ions and retards the electron movement towards the wall. In a steady-state discharge, the radial fluxes of electrons and ions are equal; i.e., an ambipolar radial flux of charge carriers with density $j_r(r)$ is established. These particles recombine on the wall with a rate that completely compensates for the volume production rate. The radial space-charge potential $V(r) = -\int_0^r E_r(r')\,dr'$ leads to a rapid decrease of the electron density $n_e(r)$ and, particularly at low pressures, of the high energy tail of the electron energy distribution with increasing r. This behavior causes a corresponding radial decrease of the production rates of excited particles and, hence, of their densities. The radial space-charge field does not supply the electrons with additional power, but it can cause a significant radial flux of electron energy toward the column center, where the power losses by electron collisions are concentrated.

2.1. *Kinetics of Electrons and Excited Atoms*

The kinetics of the electrons in the dc column plasma is determined by the space-dependent Boltzmann equation [26]

$$\mathbf{v} \cdot \nabla_{\mathbf{r}} f - \frac{e_0}{m_e} \mathbf{E} \cdot \nabla_{\mathbf{v}} f = \sum_l C_l^{\mathrm{el}}(f) + \sum_{lk} C_{lk}^{\mathrm{in}}(f) + \sum_l C_l^{\mathrm{io}}(f) \tag{1}$$

for the velocity distribution function f of the electrons with charge $-e_0$, mass m_e, and velocity $\mathbf{v}$. On the left-hand side of Eq. (1) the electric field $\mathbf{E} = E_r(r)\mathbf{e}_r + E_x\mathbf{e}_x$ is included. The impact of elastic, conservative inelastic, and ionizing collisions of electrons with neutral particles in the ground state ($l = 0$) and in excited states ($l = 1, 2, \ldots$) is taken into account by the corresponding collision integrals $C_l^{\mathrm{el}}(f)$, $C_{lk}^{\mathrm{in}}(f)$, and $C_l^{\mathrm{io}}(f)$, where k denotes the neutral particle state after an inelastic collision process. Collisions of electrons with one another and with ions can be neglected because of the low ionization degree considered. According to the axial and azimuthal homogeneity of the column plasma, the velocity distribution can be presented by the expansion

$$f\left(u, \frac{\mathbf{v}}{v}, r\right) = \frac{1}{2\pi}\left(\frac{m_e}{2}\right)^{\frac{3}{2}} \left[f_0(r, u) + f_r(r, u)\frac{v_r}{v} + f_z(r, u)\frac{v_z}{v} \right] \tag{2}$$

in spherical harmonics, which is truncated after the second term. This truncation, i.e., the so-called two-term approximation, is generally applicable if the additional consideration of

higher order terms do not considerably change the results for the first two terms. This is true in most atomic gas plasmas and in spatially inhomogeneous plasmas, if the electric field normalized on the gas pressure does not become much higher than that typically occurring in a column plasma and if the sum of cross sections of all inelastic collision processes remains considerably less than the momentum transfer cross section [27]. The latter is valid at least in the case of all inert gases and in gas mixtures with a considerable portion of inert gases. The validity of the two-term approximation to describe the electron kinetics in the column of inert gas glow discharges has also been checked by comparisons with particle simulation methods [16].

Applying (2), the Eq. (1) is reduced to a first-order differential equation system for the isotropic distribution f_0 and the anisotropic components f_r and f_z related to the radial and axial direction as functions of the kinetic energy $u = mv^2/2$ and the radial position r. The elimination of the anisotropic components leads, finally, to an elliptic differential equation for the isotropic distribution $f_0(r, u)$. The standard form of this equation is obtained when replacing the kinetic energy u of the electrons by the total energy $\varepsilon = u + w(r)$, where $w(r) = -e_0 V(r)$ represents the potential energy in the radial space-charge field. Applying the transformation

$$\tilde{f}_x(r, \varepsilon) = f_x(r, u(r, \varepsilon)), \quad x = 0, r, z \tag{3}$$

and using the abbreviation $\hat{u} \equiv u(r, \varepsilon) = \varepsilon - w(r)$, the elliptic equation for $\tilde{f}_0(r, \varepsilon)$ reads [17]

$$\frac{1}{r}\frac{\partial}{\partial r}\left[r D \frac{\partial}{\partial r}\tilde{f}_0\right] + \frac{\partial}{\partial \varepsilon}\left[(e_0 E_z)^2 D \frac{\partial}{\partial \varepsilon}\tilde{f}_0 + G\tilde{f}_0\right] - \hat{u} H \tilde{f}_0 + S_0(\tilde{f}_0) = 0. \tag{4}$$

The coefficients G, H, and K and the backscattering term S_0 in Eq. (4) are given by the expressions

$$G(r, \varepsilon) = 2\sum_l \frac{m_e}{M_l}\hat{u}^2 N_l(r) Q_l^{\mathrm{m}}(\hat{u}), \tag{5a}$$

$$H(r, \varepsilon) = \sum_{lk} N_l(r) Q_{lk}^{\mathrm{in}}(\hat{u}) + \sum_l N_l(r) Q_l^{\mathrm{io}}(\hat{u}), \tag{5b}$$

$$D(r, \varepsilon) = \frac{\hat{u}}{3\left(\sum_l N_l(r) Q_l^{\mathrm{m}}(\hat{u}) + H(r, \varepsilon)\right)}, \tag{5c}$$

$$\begin{aligned} S_0(\tilde{f}_0) = &\sum_{lk}\left(\hat{u} + u_{lk}^{\mathrm{in}}\right) N_l(r) Q_{lk}^{\mathrm{in}}\left(\hat{u} + u_{lk}^{\mathrm{in}}\right)\tilde{f}_0\left(r, \varepsilon + u_{lk}^{\mathrm{in}}\right) \\ &+ 4\sum_l \left(2\hat{u} + u_l^{\mathrm{io}}\right) N_l(r) Q_l^{\mathrm{io}}\left(2\hat{u} + u_l^{\mathrm{io}}\right)\tilde{f}_0\left(r, 2\varepsilon - w + u_l^{\mathrm{io}}\right) \\ &+ \sqrt{\frac{m_e}{2}}\sum_{lk} N_l(r) N_k(r) z_{lk}^{\mathrm{ch}} \hat{u}^{\frac{1}{2}} p_{lk}^{\mathrm{ch}}(\hat{u}). \end{aligned} \tag{5d}$$

Elastic collision processes between electrons and the lth neutral particle component of mass M_l are described by the momentum transfer cross section Q_l^m. The various types of inelastic electron collisions with the lth neutral particle component are treated by the total cross sections Q_{lk}^{in} for exciting and deexciting and Q_l^{io} for ionizing collisions; and u_{lk}^{in} and

u_l^{io} are the corresponding energy losses. The second index k denotes the neutral particle component, which is produced by the exciting and deexciting collision processes. The term $S_0(\tilde{f}_0)$ describes by means of the shifted energy arguments $\varepsilon + u_{lk}^{\mathrm{in}}$ and $2\varepsilon - w + u_l^{\mathrm{io}}$ the backscattering of electrons from higher energies caused by inelastic collisions, where the production of electrons in ionizing collisions is taken into account. In addition, the electron production in chemo-ionization processes with the rate coefficients z_{lk}^{ch} and inscattering profiles p_{lk}^{ch} as given in [17] are included.

The electron density n_e and the rate coefficients z_{lk}^{in} and z_l^{io} of exciting and ionizing electron collisions result from the integrals

$$n_e(r) = \int_{w(r)}^{\infty} \tilde{f}_0(r, \varepsilon)\hat{u}^{\frac{1}{2}}\,\mathrm{d}\varepsilon, \tag{6a}$$

$$z_{lk}^{\mathrm{in}}(r) = \frac{1}{n_e(r)}\sqrt{\frac{2}{m_e}}\int_{w(r)}^{\infty} Q_{lk}^{\mathrm{in}}(\hat{u})\,\tilde{f}_0(r, \varepsilon)\hat{u}\,\mathrm{d}\varepsilon, \tag{6b}$$

$$z_l^{\mathrm{io}}(r) = \frac{1}{n_e(r)}\sqrt{\frac{2}{m_e}}\int_{w(r)}^{\infty} Q_l^{\mathrm{io}}(\hat{u})\,\tilde{f}_0(r, \varepsilon)\hat{u}\,\mathrm{d}\varepsilon \tag{6c}$$

over the isotropic distribution $\tilde{f}_0$. According to the electron particle balance, which is a moment equation of (1) and, hence, automatically fulfilled with (1) or (4), respectively, the radial flux density j_r must satisfy the relation

$$j_r(r) = \frac{1}{r}\int_0^r P_{\Sigma}^{\mathrm{io}}(r')r'\,\mathrm{d}r', \tag{7}$$

where P_{Σ}^{io} is the total charge carrier production rate according to

$$P_{\Sigma}^{\mathrm{io}}(r) = \sum_i N_l(r)n_e(r)z_l^{\mathrm{io}}(r) + \sum_{l,k} N_l(r)N_k(r)z_{lk}^{\mathrm{ch}}. \tag{8}$$

As a consequence of the two-term expansion (2), the axial electric current I_z is given by the expression

$$I_z = 2\pi e_0^2 E_z\sqrt{\frac{2}{m_e}}\int_0^{r_w}\int_{w(r)}^{\infty} D(r, \varepsilon)\frac{\partial}{\partial\varepsilon}\tilde{f}_0\,\mathrm{d}\varepsilon\, r\,\mathrm{d}r. \tag{9}$$

The densities $N_l(r)$, $l = 1, 2, \ldots$ of the excited atom states are determined by the balance equations [17]

$$-\frac{D_l^m}{r}\frac{\mathrm{d}}{\mathrm{d}r}\left(r\frac{\mathrm{d}}{\mathrm{d}r}N_l(r)\right) + N_l(r)\left(\sum_k n_e(r)z_{lk}^{\mathrm{in}}(r) + n_e(r)z_l^{\mathrm{io}}(r) + \nu_l^{\mathrm{L}}(r)\right)$$
$$= \sum_k N_k(r)n_e(r)z_{kl}^{\mathrm{in}}(r) + P_l^{\mathrm{G}}(r) \tag{10a}$$

or

$$N_l(r)\left(\frac{1}{\tau_l}+\sum_k n_e(r)z_{lk}^{\mathrm{in}}(r)+n_e(r)z_l^{\mathrm{io}}(r)+\nu_l^{\mathrm{L}}(r)\right)=\sum_k N_k(r)n_e(r)z_{kl}^{\mathrm{in}}(r)+P_l^{\mathrm{G}}(r) \tag{10b}$$

depending on whether the lth component is a metastable or a resonance state. In Eq. (10a) the radial diffusion with the diffusion coefficient D_l^m is considered, whereas the particle loss by resonance radiation is described by the effective lifetime τ_l [28] in Eq. (10b). The loss frequency is ν_l^{L} and P_l^{G} represents the production rate of the lth component in heavy particle collision processes, including chemo-ionization processes. The special form of ν_l^{L} and P_l^{G} depends, of course, on the reaction processes considered in the specific gas as illustrated in [21]. For the treatment of a neon plasma, a number of processes as described in [29] have been considered.

The system of equations (4) and (10a, 10b) coupled via the coefficients (5a–5d) and the relations (6a–6c) represents a self-consistent model of the space-dependent electron and excited atom kinetics in the column. The input parameters of this model are the external discharge parameters (tube radius r_w, current I_z, and neutral gas concentration N_0), the electric field components E_z and $E_r(r)$, and the atomic data (particle masses, collision cross sections and rate coefficients). In addition, appropriate boundary conditions for the distribution function $\tilde{f}_0$ and the densities N_l have to be taken into account. The conditions for N_l are given in [21] and those for $\tilde{f}_0$ are detailed and extensively discussed already in [17, 20]. Only the most important condition for $\tilde{f}_0$ at the tube wall,

$$\left[-\frac{1}{K}\frac{\partial}{\partial r}\tilde{f}_0\right]_{r=r_w}=[A\exp(a\hat{u}^2)]_{r=r_w}, \tag{11}$$

shall be considered here. The left-hand side of (11) corresponds to the radial anisotropic component $\tilde{f}_r(r_w,\varepsilon)$ and, hence, the right-hand side of (11) fixes, up to the factor A, the energetic distribution of the outflowing electrons to the tube wall. This outflow has to compensate the electron production by various ionization processes in the plasma volume according to the consistent steady-state electron particle balance. Therefore, the factor A can not be freely chosen for given external discharge parameters and field components. This circumstance becomes obvious from the fact that the kinetic equation (4) and all boundary conditions for $\tilde{f}_0$ except for (11) are homogeneous with respect to $\tilde{f}_0$ at least if the small term of chemoionization; i.e., the last term in (5d), is neglected. Consequently, the solution for $\tilde{f}_0$ is largely proportional to A and this factor is finally used to adjust the solution $\tilde{f}_0$ to the given discharge current I_z according to (9). Furthermore, the factor a is applied to adapt the energy dependence of $\tilde{f}_r(r_w,\varepsilon)$ to the given discharge conditions. Unfortunately, the detailed energetic distribution of the outflowing electrons depends on the complex interplay of the plasma with the processes at the wall, which are insufficiently known up to now. However, it can be assumed that, as a consequence of space-charge confinement, close to the wall only electrons with low kinetic energy $\hat{u}$ can reach the wall and that the radial anisotropic part of their distribution has to be directed toward the wall. Hence, the function $\tilde{f}_r(r_w,\varepsilon)$ has to be positive and has to decrease very rapidly with $\hat{u}$ [17]. However, the specific choice of the exponential function in (11) and of a has only very little influence on the solution $\tilde{f}_0$ except for in the region close to the wall [20]. The specific choice of the energy dependence of $\tilde{f}_r$ in (11) is, in a sense, more natural

than the assumption of other authors [19, 24] supposing that $\tilde{f}_r$ is proportional to $\tilde{f}_0$ at $r = r_w$. The latter describes a complete or partial adsorption of outflowing electrons on the wall in the framework of the two-term approximation. However, boundary conditions, which are based on the latter assumption, often lead to incorrect numerical solutions of the elliptic problem for given discharge conditions and axial field strengths. This fact becomes obvious from the strong violation of the electron particle balance when it is verified by those incorrect solutions [19]. However, when applying condition (11) the consistent electron particle balance becomes fulfilled within the numerical accuracy for any given axial field strength and radial potential chosen in reasonable limits. Unphysical solutions have been obtained only by using a nonmonotonic radial potential, a potential with much lower or higher wall potential (by more than 30%), or a much lower or higher axial field with respect to corresponding measurements. In particular, this model of the electron kinetics and the reaction kinetics of excited neutral particles yields reasonable values for the the radial flux density $j_r(r)$ and the electron density $n_e(r)$ if the given radial space-charge field $E_r(r)$ and axial field E_z are reasonably close to the real values.

2.2. *Ion Density and Space-Charge Field*

The radial space-charge field $E_r(r)$ is determined by the Poisson equation

$$\frac{1}{r}\frac{\mathrm{d}}{\mathrm{d}r}(r E_r(r)) = \frac{e_0}{\varepsilon_0}(n_i(r) - n_e(r)), \tag{12}$$

where ε_0 is the permittivity of free space. To get the ion density $n_i(r)$, an appropriate treatment of the ion kinetics is required. The common assumption used is that the ion energy distribution is a Maxwellian with a temperature independent of the radial position and equal to the gas temperature [9]. Thus, the ion kinetics can be treated by their momentum balance equation [7–10],

$$\frac{1}{r}\frac{\mathrm{d}}{\mathrm{d}r}\left(\frac{r(j_r(r))^2}{n_i(r)}\right) - \frac{e_0 E_r(r)}{M_i} n_i(r) = -j_r(r) N_0 z^{\mathrm{cht}}, \tag{13}$$

where M_i denotes the ion mass. The first term on the left-hand side describes the ion inertia, which becomes important close to the tube wall. The right-hand side includes the action of the most important kind of ion collision processes, i.e., the charge transfer collisions between ions and neutral gas atoms with the constant rate coefficient z^{cht}. The ion diffusion term is omitted in Eq. (13) because of the low ion temperature at the considered discharge conditions. According to the symmetry of the column plasma, the conditions $E_r(0) = 0$, $j_r(0) = 0$, $\frac{\mathrm{d}}{\mathrm{d}r} n_e(r)|_{r=0} = 0$, and $\frac{\mathrm{d}}{\mathrm{d}r} n_i(r)|_{r=0} = 0$ are applied at the column center.

Equations (12) and (13) determine the space-charge field $E_r(r)$ and the ion density $n_i(r)$ for given radial flux density $j_r(r)$ and electron density $n_e(r)$. Thus, the solution of these equations coupled with the treatment of the space-dependent electron and excited atom kinetics, as detailed above, yields a self-consistent description of the space-charge confined column plasma, i.e., a description of all important plasma components and the space-charge field for given axial field strength and discharge parameters. At this point, it has to be pointed out that no relation which that fixes the axial field strength is included in the presented equation system. Consequently, the kinetics of the column plasma components and the space-charge field can be determined applying, within certain limits, various values of the axial field

strength. This means the axial field established in the steady state is determined not only by the physical processes inside the column plasma but also by the complex interplay of the plasma and the processes at the tube wall. Additional conditions have to be taken into account to self-consistently determine the axial field strength in, the dc column plasma, which may arise from a detailed description of the plasma–wall interaction, e.g., of the establishment of the surface charge and the efficiency of the charge carrier recombination at dielectric walls. The latter is not the topic of this paper. However, this task requires an accurate quantitative description of the physics in the plasma as provided by the presented model.

3. SOLUTION TECHNIQUE

The complete equation system ultimately consists of the Eqs. (4), (10a, b), (12), and (13). These equations are nonlinearly coupled by the integral expressions (6a–c) and (7) and by the coefficients (5a–d). In this section the method to solve this nonlinear equation system is presented. The system can be separated into two subsystems, namely that of (4) and (10a, b) for the treatment of the electron and excited atom kinetics and that of (12) and (13) for the determination of the ion density and the space-charge field. The structure of the entire method is illustrated by means of the scheme in Fig. 1.

The solution method used here for the treatment of the electron and excited atom kinetics, i.e., the coupled solution of (4) and (10a, b) applying appropriate boundary conditions and the normalization according to (9), has been described in detail in previous papers [17–21] and is presupposed in this paper. The basic structure is represented in the scheme in Fig. 1.

In this regard it should be additionally mentioned that instead of Eq. (4), the ordinary differential equation derived in the scope of the nonlocal approach [18, 24, 25] can be used and solved to simplify the entire solution method. This simplified approach is applicable under special discharge conditions only and yields less accurate results in comparison with a direct solution of the elliptic equation (4). However, the computation time to solve (4) is by a factor of about 10 larger than the application of the nonlocal approach. Hence, that approach has been used in addition to the strict solution for numerical studies.

At first, several techniques to solve the subsystem of Poisson's equation (12) and the ion momentum balance equation (13) coupled with the treatment of the electron and excited atom kinetics are discussed. While doing this, the known treatment of the electron and excited atom kinetics is considered to be another subsystem, which yields profiles $n_e^{\mathrm{g}}(r)$ and $j_r^{\mathrm{g}}(r)$ of the electron density and the radial flux density according to (6a) and (7) for a given radial space-charge field $E_r^{\mathrm{g}}(r)$ (or given radial potential $V^{\mathrm{g}}(r)$) as indicated in Fig. 1. Now, using $n_e^{\mathrm{g}}(r)$ and $j_r^{\mathrm{g}}(r)$, the new profiles $n_i^{\mathrm{n}}(r)$ and $E_r^{\mathrm{n}}(r)$ of the ion density and the radial space-charge field have to be determined by means of solving (12) and (13).

One way to treat the subsystem of (12) and (13) is to consider it as a system of differential equations for a given electron density $n_e^{\mathrm{g}}(r)$ and radial flux density $j_r^{\mathrm{g}}(r)$. Then, an initial value problem has to be solved for $n_i^{\mathrm{n}}(r)$ and $E_r^{\mathrm{n}}(r)$ starting from the column center with appropriate initial values. However, in this case the integration of (12) and (13) for given discrete values of $n_e^{\mathrm{g}}(r)$ and $j_r^{\mathrm{g}}(r)$ often diverges after a few integration steps. This can be attributed to a stronger deviation of $n_i^{\mathrm{n}}(r)$, obtained from the momentum balance, from $n_e^{\mathrm{g}}(r)$, which is fixed and belongs to the given field $E_r^{\mathrm{g}}(r)$. But already small differences between $n_e^{\mathrm{g}}(r)$ and $n_i^{\mathrm{n}}(r)$ lead to large variations of the radial field $E_r^{\mathrm{n}}(r)$, according to Poisson's equation, and can produce a divergence of the numerical solution.

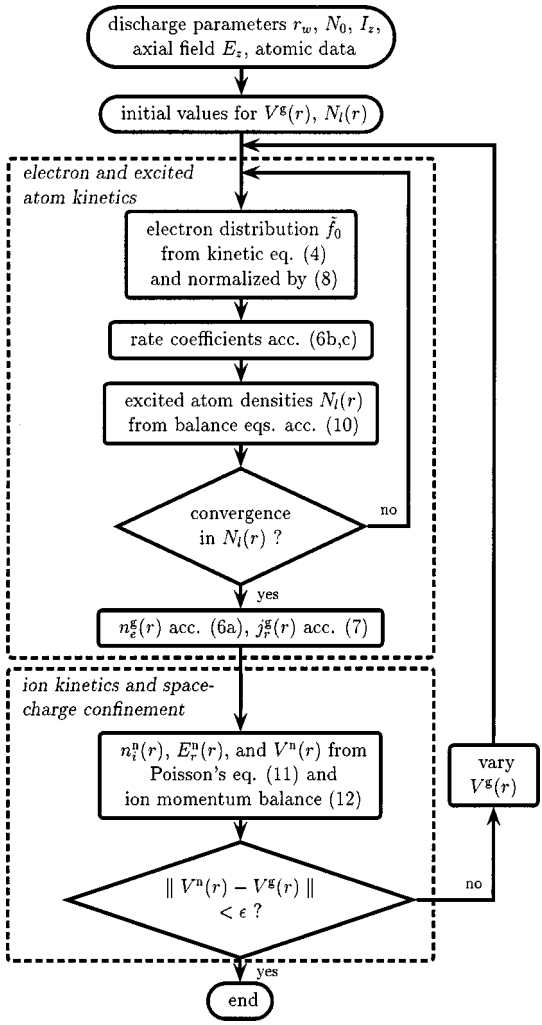

FIG. 1. Scheme of the self-consistent positive column model.

To avoid the amplification of small deviations of the densities by Poisson's equation, an alternative treatment of the subsystem of (12) and (13) has been chosen. The Poisson equation (12) is used to calculate the profile $n_i^n(r)$ of the ion density for the given electron density $n_e^g(r)$ and the given radial field $E_r^g(r)$. Then $n_i^n(r)$ and the given $j_r^g(r)$ are applied in the ion momentum balance to get a new $E_r^n(r)$. Hence, the specific arrangement

$$n_i^n(r) = n_\varepsilon^g(r) + \frac{\varepsilon_0}{e_0 r}\frac{\mathrm{d}}{\mathrm{d}r}\left(r E_r^g(r)\right), \tag{14a}$$

$$E_r^n(r) = \frac{M_i}{n_i^n(r) e_0}\left(\frac{1}{r}\frac{\mathrm{d}}{\mathrm{d}r}\left(\frac{r\left(j_r^g(r)\right)^2}{n_i^n(r)}\right) + j_r^g(r) N_0 z^{\mathrm{cht}}\right), \tag{14b}$$

$$V^n(r) = -\int_0^r E_r^n(r')\,\mathrm{d}r' \tag{14c}$$

of the equation system is used to determine the new profile $V^n(r)$ of the radial potential.

The consistent solution of both subsystems and the corresponding profile of the radial potential are found if ultimately the given potential $V^{\mathrm{g}}(r)$ and its new profile $V^{\mathrm{n}}(r)$ coincide; i.e., the relation $V^{\mathrm{g}}(r) = V^{\mathrm{n}}(r)$ holds for all radial positions. The corresponding numerical task is to find such a potential function $V^{\mathrm{g}}(r)$ for which the distance between $V^{\mathrm{n}}(r)$ and $V^{\mathrm{g}}(r)$ becomes sufficiently small. To assess the distance, an appropriate norm function

$$h = \|V^{\mathrm{n}}(r) - V^{\mathrm{g}}(r)\| \tag{15}$$

has to be chosen. Here, either the mean relative error h^{rel}, the maximum norm $h^{\max}$, or the Euclidean norm h^{Eucl}, according to the expressions

$$h^{\mathrm{rel}} = \frac{1}{m}\sum_{i=1}^{m}\frac{|V^{\mathrm{n}}(r_i) - V^{\mathrm{g}}(r_i)|}{|V^{\mathrm{g}}(r_i)|}, \tag{16a}$$

$$h^{\max} = \max_{1\le i\le m}|V^{\mathrm{n}}(r_i) - V^{\mathrm{g}}(r_i)|, \tag{16b}$$

$$h^{\mathrm{Eucl}} = \sqrt{\sum_{i=1}^{m}(V^{\mathrm{n}}(r_i) - V^{\mathrm{g}}(r_i))^2}, \tag{16c}$$

is considered. The expressions are related to the discretization of the radial potential profile applying m radial positions r_i.

Further on, different numerical methods to find a consistent solution of both subsystems, i.e., to minimize h, are discussed.

3.1. *Iterative Methods*

An often used method is an iterative treatment of the subsystems, i.e., starting the kth iteration with the given radial potential $V^{\mathrm{g}}(r) = V^{(k)}(r)$ and the corresponding radial field, solving the subsystem of the electron and excited atom kinetics to get $n_e^{(k)}(r)$ and $j_r^{(k)}(r)$, which are then used in (14) instead of $n_e^{\mathrm{g}}(r)$ and $j_r^{\mathrm{g}}(r)$ to calculate $n_i^{(k+1)}(r)$ and the new functions $E_r^{(k+1)}(r)$ and $V^{(k+1)}(r)$. In the next iteration $V^{\mathrm{g}}(r) = V^{(k+1)}(r)$ and $E_r^{\mathrm{g}}(r) = E_r^{(k+1)}(r)$ are used as the given radial potential and field. The iterative procedure is terminated if the distance between $V^{(k+1)}(r)$ and $V^{(k)}(r)$ is sufficiently small. In some cases, iterative methods converge very fast and can lead to a sufficiently accurate result after about 10 iterations [24]. However, in the case considered here, a divergence of the iterative method has been generally found for different discharge conditions. The divergence cannot be prevented by an appropriate blending, i.e., by applying $V^{\mathrm{g}}(r) = \omega V^{(k+1)}(r) + (1-\omega)V^{(k)}(r)$ in the $(k+1)$th iteration, where $0 < \omega \le 1$ is the blending factor. As an example, the development of the potential function of a neon column-plasma with radius $r_w = 1.7$ cm, pressure $p_0 = 74.5$ Pa, discharge current $I_z = 10$ mA, axial field strength $E_z = 2.12$ V/cm, and with $\omega = 0.1$, can be seen in Fig. 2. The potential profile, are compared with that self-consistent potential, which is the result of a successful solution by means of an optimization technique as explained at the end of this section.

3.2. *Basic Aspects of Optimization*

A more appropriate way is to use a nonlinear optimization technique to modify a given potential profile $V^{\mathrm{g}}(r)$ so that the distance h according to (15) becomes sufficiently small. Therefore, $V^{\mathrm{g}}(r)$ and h have to be expressed as functions of a number of parameters. Knowing that polynomials are excellent approximations of radial potential profiles obtained

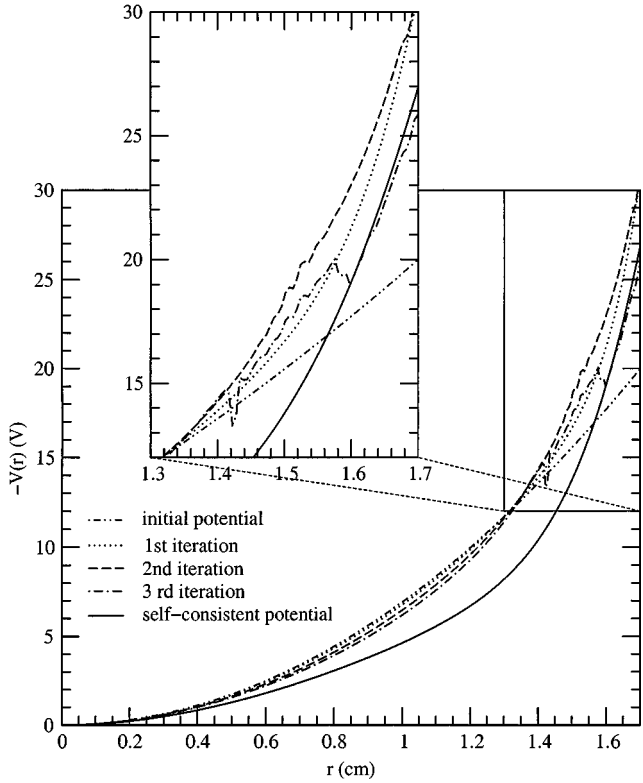

FIG. 2. Courses of the radial space-charge potential obtained by a simple iterative treatment in comparison with the self-consistent potential.

by probe measurements [18], a polynomial of the reduced radial position r/r_w and of the order $15 \leq n \leq 30$ with the parameter vector $\mathbf{a} = (a_1, \ldots, a_n) \in \mathbb{R}^n$ has been used to parameterize the given potential profile and the norm function according to

$$V^{\mathrm{g}}(r, \mathbf{a}) = a_1 \left(\frac{r}{r_w}\right)^2 + a_2 \left(\frac{r}{r_w}\right)^4 + a_3 \left(\frac{r}{r_w}\right)^5 + \cdots + a_n \left(\frac{r}{r_w}\right)^{n+2}, \tag{17a}$$

$$h(\mathbf{a}) = \|V^{\mathrm{n}}(r) - V^{\mathrm{g}}(r, \mathbf{a})\|. \tag{17b}$$

The terms of orders 0, 1, and 3 are omitted because of the natural choice $V^{\mathrm{g}}(0, \mathbf{a}) = 0$ and the symmetry conditions $-\frac{\mathrm{d}}{\mathrm{d}r} V^{\mathrm{g}}(r, \mathbf{a})|_{r=0} = E_r^{\mathrm{g}}(0, \mathbf{a}) = 0$ and $-\frac{\mathrm{d}}{\mathrm{d}r}[\frac{1}{r}\frac{\mathrm{d}}{\mathrm{d}r}(r\frac{\mathrm{d}}{\mathrm{d}r} V^{\mathrm{g}}(r, \mathbf{a}))]|_{r=0} \sim \frac{\mathrm{d}}{\mathrm{d}r}(n_i^{\mathrm{n}}(r) - n_e^{\mathrm{g}}(r))|_{r=0} = 0$. The aim of a nonlinear optimization technique is to systematically minimize the norm-functional $h(\mathbf{a})$ by varying the coefficients $a_1, \ldots, a_n$. Therefore, it is necessary for every potential $V^{\mathrm{g}}(r, \mathbf{a})$, which belongs to a specific $\mathbf{a}$, to solve the subsystem of the electron and excited atom kinetics, as well as the subsystem (14), to obtain the corresponding $V^{\mathrm{n}}(r)$ and $h(\mathbf{a})$. Generally, there exist two main strategies to find the minimum of the functional $h(\mathbf{a})$. The first determines a descent direction aided by a gradient evaluation with the aim of performing a search in this direction in every optimization step. The second performs a multidirectional search, and this one is often applicable if $h(\mathbf{a})$ is discontinuous or even if the function values are "noisy." Both variants are treated and discussed in detail in the following to assess their suitability. In particular, algorithms that can be adapted to run the optimization on parallel computers are considered.

3.3. *Assessment of Various Optimization Techniques*

If we assume that $h(\mathbf{a})$ has continuous second partial derivatives with respect to all of its variables, then a gradient method such as the finite difference Newton method, the quasi-Newton method [30–34], or at least a variation of these, could be applied. The scheme of the finite difference Newton method is to calculate from a starting point a Newton direction and to perform a line search until one reaches the minimum in that direction. The minimum point is now chosen as the new starting point. The Newton direction is obtained from the first- and second-order partial derivatives using finite differences. The advantage of gradient methods is that they often need fewer optimization steps than multidirectional search algorithms, but the numerical cost of every step is at least twice as high.

Among the multidirectional minimum-search algorithms, two methods, a modified minimum-search algorithm in the $\mathbb{R}^n$ adapted from Hooke and Jeeves (see [35]) and the downhill simplex method from Nelder and Mead [36, 34], have been considered.

The minimum-search algorithm varies all components of $\mathbf{a}$ with a fixed step size until $h(\mathbf{a})$ reaches the minimum. Then the step size is shortened and a new search starts.

The downhill simplex method is based on moving a nondegenerate simplex around the space $\mathbb{R}^n$, changing its size but not its shape. The nondegenerate simplex is formed by the point $\mathbf{a}$ and additional n points resulting from the variation of each coordinate of $\mathbf{a}$. The movement of the simplex is managed in such a way that the neighborhood of the corner point with the smallest value of h is examined systematically in each case and that the value of h converges to a minimum during the movement. For this, the simplex is compressed, expanded, or reflected at the corner point with the smallest value of h, and the function h is calculated for each of the other corner points of the simplex in every step. The advantage of the downhill simplex method is that it is relatively robust against cycles in the variation of $\mathbf{a}$ and against falling into a local minima of the functional $h(\mathbf{a})$.

These three minimum-search algorithms have been implemented and checked. Here, all three different norm functions have been used alternatively for $h(\mathbf{a})$ to regulate the variation of $\mathbf{a}$ and to check the convergence. It has turned out that the mean relative error is the best norm function to steer the minimum-search algorithm, i.e., to vary $\mathbf{a}$ in such way that the algorithm finds an optimum course to the minimum point. However, the Euclidean norm is the most suitable norm function to steer the downhill simplex method and the finite difference Newton method. The maximum norm is the appropriate one to assess the convergence of the radial potential function and to break off the search algorithms, because the maximum error mostly appears at radial positions very near the column wall, where the potential profile strongly influences the radial flux of charge carriers toward the wall.

Figure 3 shows typical progressions of the three norm functions over a range of 500 optimization steps for the three different minimum-search algorithms. Here, a potential function according to (17a) with $n = 20$ has been used and the same discharge situation as in Fig. 2 has been treated. The finite difference Newton method yields a considerable error reduction after about 40 steps but then comes into a saturation range with a very slow improvement of the potential function. In particular, the mean relative error and the Euclidean norm are much higher than for the other methods after 500 steps. The saturation in the error reduction is a typical behavior of the finite difference Newton method and indicates that a local minimum instead of a global minimum in the functional $h(\mathbf{a})$ has been found. The minimum-search algorithm in Fig. 3b leads to very small values of all three norms already after about 100 steps. However, during further steps the norm functions slightly increase

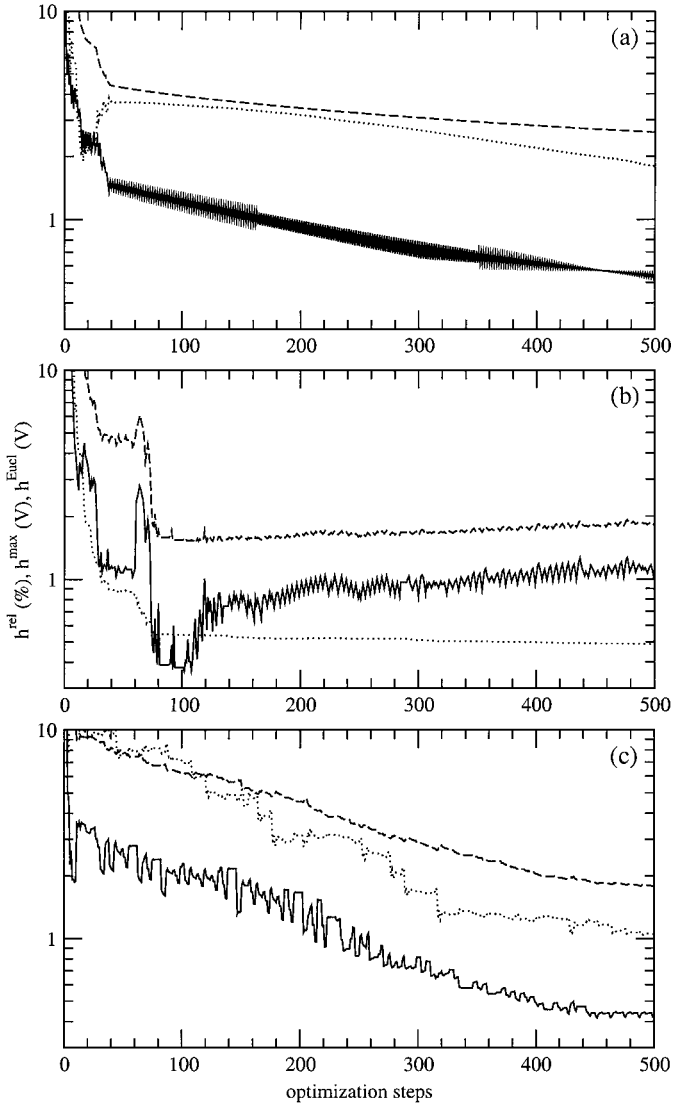

FIG. 3. Courses of the maximum norm h^{max} (solid line), the Euclidean norm h^{Eucl} (dashed line), and the mean relative error h^{rel} (dotted line) related to 300 radial positions over 500 optimization steps of the finite difference Newton method (a), the minimum-search algorithm (b), and the downhill simplex method (c).

except for the mean relative error, which has been used to steer the potential variation in that method. A disadvantage of the minimum-search algorithm is the irregularity of the error reduction, which leads to a cyclic behavior of the potential variation in some cases. The most continuous decrease of the norm functions has been obtained by the downhill simplex method, which can be seen in Fig. 3c. This method leads after 500 steps to the smallest maximum norm, which is the most significant one to assess the improvement of the potential profile. The continuous error decrease indicates the stability of that method, which, among the three methods, most rarely comes into a saturation of the potential variation. An additional advantage of the multidirectional minimum-search algorithms in comparison with Newton-like methods is that one step in the downhill simplex method as well as in

the minimum-search algorithm needs half as much steps of evaluation of a new potential profile by treating each time the electron and excited atom kinetics and applying (14). Consequently, the downhill simplex method is the most stable and efficient method for finding a consistent solution for the radial potential.

Additionally, the achieved accuracy of the result, strongly depends on the model function used for $V^{g}(r, \mathbf{a})$. Sufficient accuracy in the adjustment of the radial potential, i.e., a mean relative error of less then 0.1% and a maximum norm of less then 0.1 V (which means about 0.5% of the radial potential at the wall), can be reached using polynomial functions according to (17a) of an appropriate order. In Fig. 4 the dependence of the three norm progressions for the downhill simplex method on the number of coefficients and on the

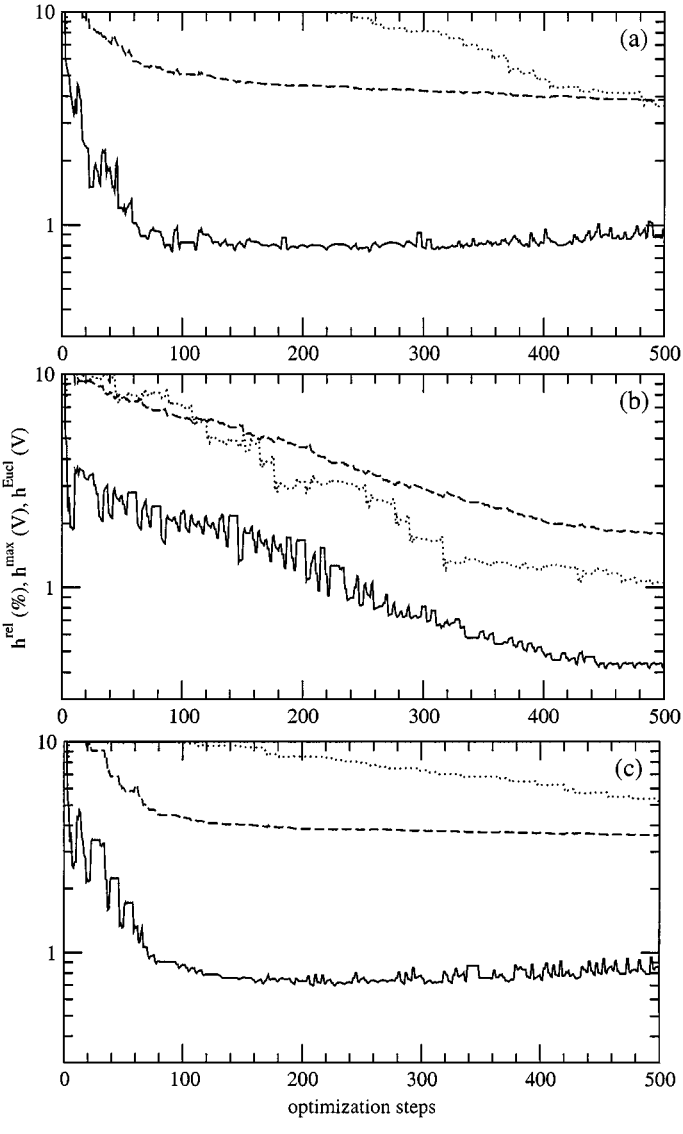

FIG. 4. Courses of norm functions as in Fig. 3 over 500 optimization steps of the downhill simplex method where a polynomial function with 16 coefficients (a), with 20 coefficients (b), and with 30 coefficients (c) has been used for $V^{g}(r, \mathbf{a})$.

chosen powers of the polynomial are demonstrated as in Fig. 3. A polynomial with $n = 20$ and 20 coefficients has been used in Fig. 4b and a polynomial with $n = 30$ and 30 coefficients has been considered in Fig. 4c. In Fig. 4a, a polynomial according to (17a) with $n = 20$ (however, without the terms involving the coefficients a_{12}, a_{13}, a_{16}, and a_{17}, and therefore with only 16 coefficients) has been used. It can be seen that only in the case of 20 coefficients a continuous decrease of all norm functions over 500 optimization steps has been obtained. Finally, a maximum norm of about 0.4 V has been reached. In the case of 16 coefficients, after the first 100 steps no further reduction of the maximum norm and, hence, no further improvement of the radial potential function could be reached because of the insufficient model function. The norm progressions in Fig. 4c, belonging to the case of 30 coefficients, look similar to those in Fig. 4a. However, the insufficient error reduction over 500 steps in this case is presumably caused by the greater effort of the function minimization in the 30-dimensional space.

4. ILLUSTRATIVE RESULTS

In this section, results obtained by the method elucidated in the preceding section will be presented. As an example, again the neon dc discharge at 74.5 Pa pressure in a tube with the radius 1.7 cm is considered. For a discharge current of 10 mA an axial electric field strength of $E_z = 2.12$ V/cm in the column plasma has been found by electrical probe measurements [18].

The radial space-charge potential has been self-consistently adjusted using the downhill simplex method and a polynomial with 20 coefficients according to (17a). The radially inhomogeneous electron kinetics within this method has been treated by strictly solving the elliptic Eq. (4) as well as by applying instead of (4) the above mentioned nonlocal approach.

The corresponding results for the radial space-charge potential $V(r)$ are shown in Fig. 5. The results have been obtained using the axial field strength $E_z = 2.12$ V/cm according to the measurements. The potential profile obtained by applying the nonlocal approach exceeds the profile obtained by solving Eq. (4) particularly in the region near the tube wall. This discrepancy results mainly from the overestimation of the charge carrier production and, hence, of the density j_r of the radial ambipolar flux of charge carriers by the nonlocal approach, which have been extensively discussed already in previous papers [18, 25]. The latter can be clearly seen from the corresponding profiles of j_r presented additionally in Fig. 5.

In Figs. 6 and 7 the densities of the most important particle components in the noon plasma, i.e., of electrons, ions, and atoms in the lower excited states, and the rate coefficients of important electron collision processes are shown as functions of the radial position. These quantities are related to the radial potential displayed in Fig. 5 by the solid line and have been obtained by the self-consistent description including Eq. (4). In particular, the densities of the resonance states s_4 and s_2 strongly decrease with increasing radial position. Larger deviations between the electron and ion density have been found in the range from about 80% of the tube radius onward. The strong radial decrease of important electron collision rate coefficients, in particular, those of excitation and ionization of the ground state neon atoms with increasing radial position, indicates the pronouncedly nonlocal behavior of the neon plasma at the considered pressure.

If the value of the axial field strength E_z is changed around the measured axial field of 2.12 V/cm, a sensitive dependence of the radial potential on E_z is obtained. Figure 8 shows the profiles of $V(r)$ obtained by the self-consistent description including Eq. (4) for three

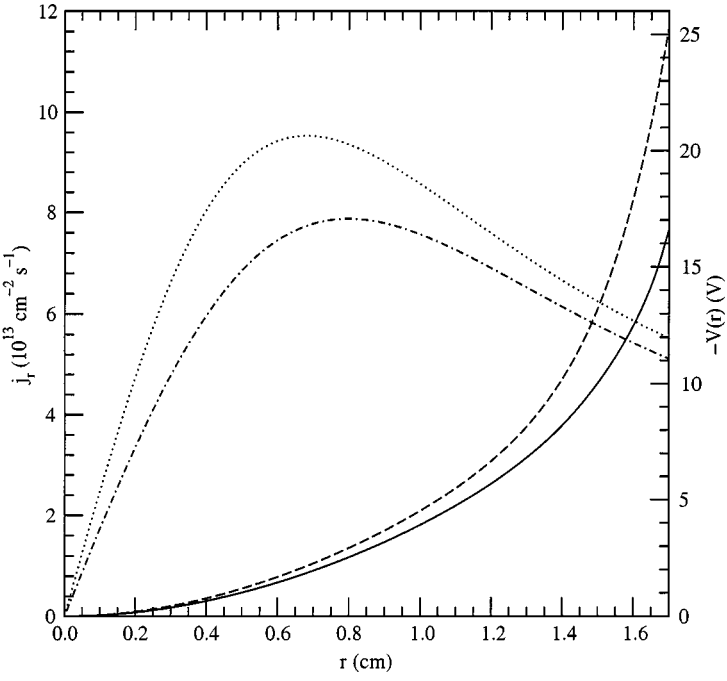

FIG. 5. Radial space-charge potential $V(r)$ and radial flux density j_r of the charge carriers from the self-consistent description by strictly solving Eq. (4) (solid and dash-dotted line) and by applying the nonlocal approach (dashed and dotted line).

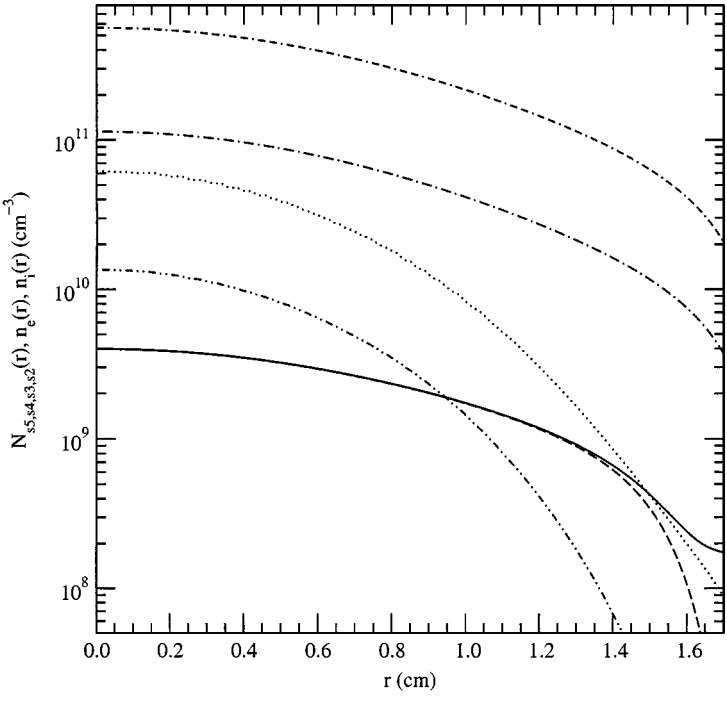

FIG. 6. Densities $n_i(r)$ of neon ions (solid line), $n_e(r)$ of electrons (dashed line), $N_{s5}(r)$ (dash-dash-dotted line) and $N_{s3}(r)$ (dash-dotted line) of metastable neon atoms and $N_{s4}(r)$ (dotted line) and $N_{s2}(r)$ (dash-dot-dotted line) of neon atoms in the lower resonance states.

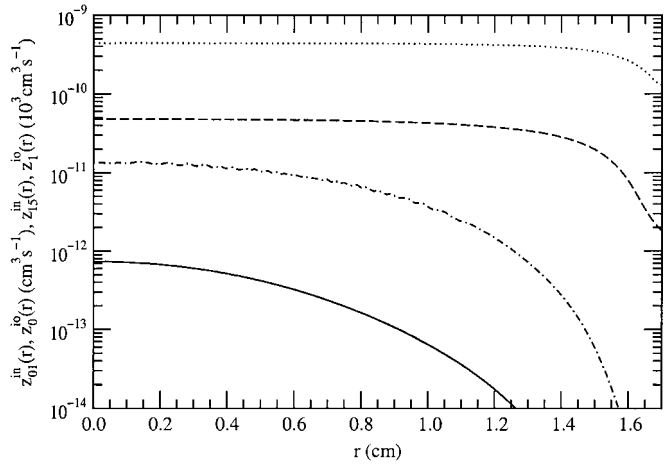

FIG. 7. Radial courses of the electron collision rate coefficients z_0^{io} of the ionization of ground state neon atoms (solid line), z_1^{io} of the ionization of the lowest metastable $s5$-state (dashed line), z_{01}^{in} of the excitation of ground state neon atoms to the lowest metastable $s5$-state (dash-dotted line), and z_{15}^{in} of the excitation of the lowest metastable $s5$-state to higher excited p-states (dotted line).

values of E_z, in comparison with the radial potential found by probe measurements [18]. Notice that for all these different values of the axial field, reasonable results for the plasma properties, in particular for the electron kinetic quantities, have been obtained. The accuracy of the results has been checked by, among other things, the fulfillment of the electron particle

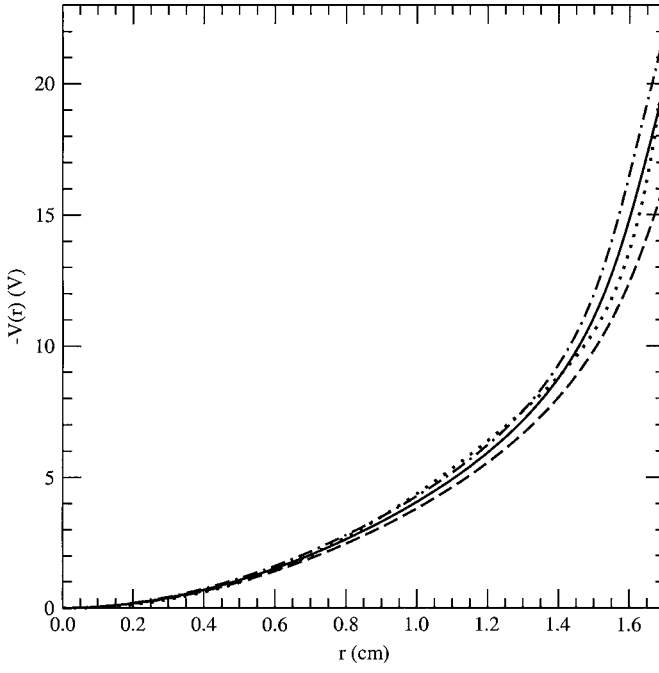

FIG. 8. Radial space-charge potential $V(r)$ from the self-consistent description by strictly solving Eq. (4) and applying the values 2.1 (dashed line), 2.2 (solid line), and 2.3 V/cm (dash-dotted line) of the axial field E_z in comparison with the result of probe measurements (dotted line).

and power balance. Here, the numerical deviations from the fulfillment amount to less than 2% in the particle balance and less than 0.5% in the power balance. It becomes obvious from Fig. 8 that quite good agreement between the measurements and the theoretical result for $E_z = 2.2$ V/cm has been reached.

Consequently, the presented method for the self-consistent description allows a rather accurate determination of the radial space-charge potential if an appropriate value of the axial field strength is given and the relevant atomic data are known with sufficient accuracy.

5. CONCLUSION

A method for the self-consistent description of radial space-charge potential and kinetics of the plasma components in the cylindrical axially homogeneous column plasma of dc discharges has been developed. The treatment of the nonlocal kinetics of the electron component is based on the solution of the relevant radially inhomogeneous kinetic equation applying a two-term expansion of the electron velocity distribution. The densities of the excited neutral particles in the plasma are determined by their particle balances. The ion momentum balance and the Poisson equation are used to calculate the ion density and the radial potential.

Several techniques to solve self-consistently these nonlinearly coupled equations have been applied and assessed concerning their convergence and applicability. The techniques used are based on the iterative improvement or optimization of the radial profile of the radial space-charge potential. In the scope of these techniques, in every step the electron and excited particle kinetics are consistently treated for a given radial potential, which yields, especially, corresponding radial profiles for the electron density and the density of the radial ambipolar flux. Using these densities, a new potential is obtained applying the ion momentum balance and Poisson's equation. The given potential profiles have been varied and the treatment of the plasma components has been repeated until the new potential sufficiently coincides with the given potential. It has been found that the iterative adjustment of the radial potential, i.e., taking the new potential, as the given potential in the next step, is inapplicable to solving the relevant nonlinear equation system. Appropriate methods to find the self-consistent radial potential are function minimization techniques such as gradient methods or multidirectional minimum-search algorithms. These techniques have been used to optimize the coefficients of an appropriate polynomial representation of the radial potential in such a way that the distance between the polynomial and the corresponding new potential approaches a minimum. The downhill simplex method of Nelder and Mead [36] with an appropriate steering using the Euclidean norm has turned out to be the most stable and suitable technique for optimizing the radial potential profile.

Initial results of the method for the column plasma of a neon dc discharge at a pressure of 74.5 Pa have been presented to illustrate the power of this optimization technique. The axial electric field strength has an unexpectedly sensitive influence on the radial space-charge potential. Furthermore, it could be clearly shown that the use of the nonlocal approach to treat the radially inhomogeneous electron kinetics instead of the strict kinetic treatment leads to a noticeable enhancement of the radial potential course especially in the outer column region.

By using the new method it could be demonstrated that a steady state of a column plasma, including the space-charge confinement (i.e., reasonable solutions for the electron quantities, the densities of ions and excited atoms, and the space-charge field) can be self-consistently

determined for several in reasonable limits given values of the axial field strength. This fact means that the steady state of a column plasma and, in particular, the axial field established in the steady state, is not sufficiently determined by the involved basic equations of the kinetics of plasma components inside the column. Additional conditions have to be taken into account that answer the question of what happens when the charge carriers reach the wall. Such conditions may eventually result from a detailed description of plasma–wall interaction processes, in particular of the adsorption and recombination of charge carriers and the establishment of the negative surface charge at the wall. In this respect, additional effort has to be undertaken to elaborate the basic physical mechanisms, which determine the axial field strength, and to deduce the appropriate conditions. However, the presented method is a necessary and important step for such an extended investigation and for the development of a complete self-consistent description of the column plasma, including its interaction with the discharge tube wall.

REFERENCES

1. W. Schottky, Wandströme und Theorie der positiven Säule, Diffusionstheorie der positiven Säule, *Z. Phys.* **25**, 342, 635 (1924).
2. S. A. Self and H. N. Ewald, Static theory of a discharge column at intermediate pressures, *Phys. Fluids* **9**, 2486 (1966).
3. H. W. Friedman, Nonlinear asymptotic analysis of the positive column, *Phys. Fluids* **10**, 2053 (1967).
4. J. Behnke, Yu. B. Golubovskii, S. U. Nisimov, and I. A. Porokhova, Self-consistent model of a positive column in an inert gas discharge at low pressure and small currents, *Contrib. Plasma Phys.* **36**, 75 (1996).
5. W. P. Allis and D. J. Rose, The transition from free to ambipolar disffusion, *Phys. Rev.* **93**, 84 (1954).
6. I. M. Cohen and M. D. Kruskal, Asymptotic theory of the positive column of a gas discharge, *Phys. Fluids* **8**, 920 (1965).
7. J. R. Forrest and R. N. Franklin, The theory of the positive column including space-charge effects, *J. Phys. D* **1**, 1357 (1968).
8. J. H. Ingold, Two-fluid theory of the positive column of a gas discharge, *Phys. Fluids* **8**, 920 (1972).
9. A. Metze, D. W. Ernie, and H. J. Oskam, Radial distributions of charged-particle densities and electric field strength in the positive column, *Phys. Rev. A* **39**, 4117 (1989).
10. J. F. Behnke, T. Bindemann, H. Deutsch, and K. Becker, Wall recombination in a glow discharge, *Contrib. Plasma Phys.* **37**, 345 (1997).
11. J. Wilhelm and R. Winkler, Zur Theorie der subnormalen Säule einer Niederdruck-Glimmentladung, *Contrib. Plasma Phys.* **7**, 97 (1967).
12. J. H. Ingold, Nonequilibrium positive column, *Phys. Rev. E* **56**, 5932 (1997).
13. M. J. Hartig and M. J. Kushner, Radially dependent solutions of Boltzmann's equation in low-temperature plasmas using a modified two-term expansion, *J. Appl. Phys.* **73**, 1080 (1993).
14. G. J. Parker, W. N. G. Hitchon, and J. E. Lawler, Numerical solution of the Boltzmann equation in cylindrical geometry, *Phys. Rev. E* **50**, 3210 (1994).
15. C. Busch and U. Kortshagen, Numerical solution of the spatially inhomogeneous Boltzmann equation and verification of the nonlocal approach for an argon plasma, *Phys. Rev. E* **51**, 280 (1995).
16. U. Kortshagen, G. J. Parker, and J. E. Lawler, Comparison of Monte Carlo simulations and nonlocal calculations of the electron distribution function in a positive column plasma, *Phys. Rev. E* **54**, 6746 (1996).
17. D. Uhrlandt and R. Winkler, Radial structure of the kinetics and production of electrons in the dc column plasma, *Plasma Chem. Plasma Process* **16**, 517 (1996).
18. S. Pfau, J. Rohmann, D. Uhrlandt, and R. Winkler, Experimental and theoretical study of the inhomogeneous electron kinetics in the dc column plasma, *Contrib. Plasma Phys.* **36**, 449 (1996).

19. L. L. Alves, G. Gousset, and C. M. Ferreira, Self-contained solution to the spatially inhomogeneous electron Boltzmann equation in a cylindrical plasma column, *Phys. Rev. E* **55**, 890 (1997).
20. R. Winkler and D. Uhrlandt, On the radial structure of the electron velocity distribution and related macroscopic properties in dc column plasmas, in Electron Kinetics and Applications of Glow Discharges, edited by U. Kortshagen and L. D. Tsendin, NATO ASI Series (Plenum Press, New York, 1998), Vol. 369, pp. 119–136.
21. H. Lange, F. Leipold, M. Otte, S. Pfau, and D. Uhrlandt, Spatially dependent kinetics of electrons and excited atoms in the column plasma of a He–Xe dc discharge, *Plasma Chem. Plasma Process* **19**(2), 255 (1999).
22. Yu. B. Golubovskii, I. A. Porokhova, J. Behnke, and J. F. Behnke, A comparison of kinetic and fluid models of the positive column of discharges in inert gases, *J. Phys. D Appl. Phys.* **32**, 456 (1999).
23. Yu. B. Golubovskii, V. O. Nekuchaev, and I. A. Porokhova, Electron kinetics in inhomogeneous and stratified positive column and anode region, in Electron Kinetics and Applications of Glow Discharges, edited by U. Kortshagen and L. D. Tsendin, NATO ASI Series (Plenum Press, New York, 1998), Vol. 369, pp. 137–160.
24. U. Kortshagen, C. Busch, and L. D. Tsendin, On simplifying approaches to the solution of the Boltzmann equation in spatially inhomogeneous plasmas, *Plasma Sources Sci. Technol.* **5**, 1 (1996).
25. M. Schmidt, D. Uhrlandt, and R. Winkler, Extension of the nonlocal approach to evaluate the electron velocity distribution, *IEEE Trans. Plasma Sci.* **27**, 1271 (1999).
26. R. Winkler, F. Sigeneger, and D. Uhrlandt, Nonlocal behaviour of the electron component in nonequilibrium plasmas, *Pure Appl. Chem.* **68**, 1065 (1996).
27. G. Petrov and R. Winkler, Multi-term treatment of electron kinetics in inhomogeneous nonequilibrium plasmas, *J. Phys. D Appl. Phys.* **30**, 53 (1997).
28. S. Pfau and R. Winkler, Das diffusionsbestimmte Plasma der positiven Säule von Nieder-druckentladungen in Neon bei mittleren Ionisierungsgraden von 10^{-8}–10^{-3}, *Contrib. Plasma Phys.* **20**, 343 (1980).
29. L. W. G. Steenhuijsen, Investigations of afterglows of neon gas discharges, *Contrib. Plasma Phys.* **21**, 301 (1981).
30. C. G. Broyden, The convergence of a class of double rank minimization algorithms, *Inst. Math. Appl.* **6**, 76, 222 (1970).
31. R. Fletcher, A new approach to variable metric algorithms, *Comput. J.* **13**, 317 (1970).
32. D. Goldfarb, A family of variable methods derived by variational means, *Math. Comput.* **24**, 23 (1970).
33. D. F. Shanno, Conditioning of quasi-newton methods for function minimization, *Math. Comput.* **24**, 647 (1970).
34. T. L. Freeman and C. Phillips, *Parallel Numerical Algorithms* (Prentice Hall International, Englewood Cliffs, NJ, (1992).
35. I. N. Bronstein and K. A. Semendjajew, Ergänzende Kapitel zu Taschenbuch der Mathematik (Teubner, Leipzig, 1988).
36. J. A. Nelder and R. Mead, A simplex method for function minimization, *Comput. J.* **7**, 308 (1965).